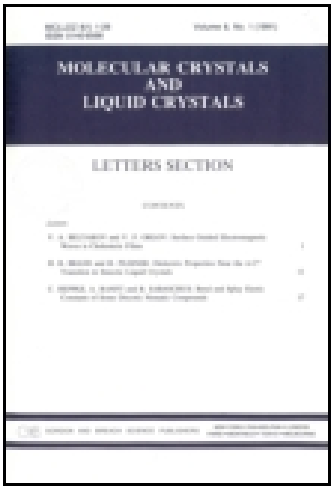

Molecular Crystals and Liquid Crystals
Publication details, including instructions for authors and subscription information:
http://www.tandfonline.com/loi/gmcl20

Precise Lens-On-Lens Architecture Using Selective Wettability for Image-Depth Representation

Se-Um Kim[a], Jiyoon Kim[a] & Sin-Doo Lee[a]
[a] School of Electrical Engineering, Seoul National University, Kwanak, Seoul, Korea
Published online: 30 Sep 2014.

To cite this article: Se-Um Kim, Jiyoon Kim & Sin-Doo Lee (2014) Precise Lens-On-Lens Architecture Using Selective Wettability for Image-Depth Representation, Molecular Crystals and Liquid Crystals, 595:1, 50-54, DOI: 10.1080/15421406.2014.917781

To link to this article: http://dx.doi.org/10.1080/15421406.2014.917781

Mol. Cryst. and Liq. Cryst., Vol. 595: pp. 50–54, 2014

ISSN: 1542-1406 print/1563-5287 online
DOI: 10.1080/15421406.2014.917781

Taylor & Francis
Taylor & Francis Group

Precise Lens-On-Lens Architecture Using Selective Wettability for Image-Depth Representation

SE-UM KIM, JIYOON KIM, AND SIN-DOO LEE*

School of Electrical Engineering, Seoul National University, Kwanak, Seoul, Korea

We demonstrate a precise lens-on-lens architecture using the concept of the selective wettability for the image-depth representation. Two focal lengths realized by the difference between two geometrical curvatures of the primary convex lens and the secondary convex lens in a lens-on-lens manner enable to produce two image planes. Such lens architecture was spontaneously produced through the selective wetting process of a photo-reactive polymer during dip-coating, followed by the irradiation of ultraviolet light for polymerization. Our selective wettability approach is capable of building various sizes and shapes of the lens-on-lens patterns over large-area without using a photo-lithography or a wet-chemical etching process.

Keywords Lens-on-lens; selective wettability; image-depth; photo-reactive polymer

1. Introduction

A variety of lens arrays with different structures have been widely used for many optical devices and systems such as autostereoscopic displays [1, 2], integral imaging displays [3–5], confocal microscopes [6, 7], a light diffuser [8], and an optical waveguide [9]. Many different methods, for example, thermal reflow [10–12], inkjet printing [13, 14], lithography [15, 16], and molding [17–19], have been suggested for fabricating lens array. The existing lens arrays produced by such methods have only a single focal length which is either fixed or tunable. Nowadays, the need of the lens arrays with the dual focusing capability has increased for potential applications in a dual-focusing optical head [20], high fill-factor image sensors [21, 22], and real-time detection of the unconfined or fluctuating targets in a lab-on-a-chip [23]. However, only a few attempts to construct the dual lens structures for the representation of the image-depth have been made so far [23–25].

In this work, we demonstrate a precise lens-on-lens architecture through a simple and versatile fabrication process based on the selective wettability [26, 27]. This approach does not require any additional complicated processes such as photo-lithography or wet-chemical etching. The repetition of the dip-coating process of a photo-reactive polymer and the subsequent ultraviolet (UV) irradiation for photo-polymerization were used

*Address correspondence to Prof. Sin-Doo Lee, School of Electrical Engineering, Seoul National University, Kwanak P.O. Box 34, Seoul 151-600, Republic of Korea. Tel.: +82-2-880-1823; Fax: +82-2-874-9769; E-mail: sidlee@plaza.snu.ac.kr

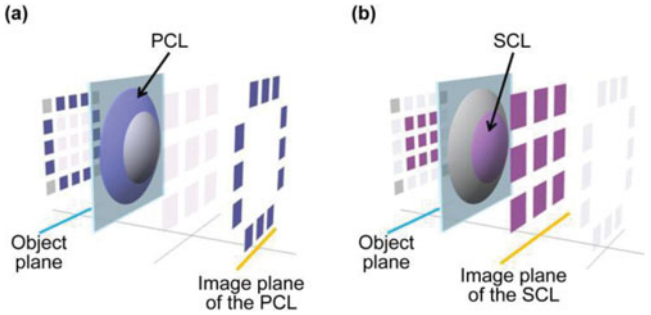

Figure 1. Schematic diagrams showing the image-depth representation principle of the lens-on-lens architecture by (a) the PCL and (b) the SCL.

for successively constructing the primary convex lens (PCL) and the secondary convex lens (SCL) onto the PCL. The image-depth representation principle of the lens-on-lens architecture, resulting from the difference between two focal lengths, is schematically shown in Fig. 1.The PCL and the SCL have two different focal planes to represent the image-depth.

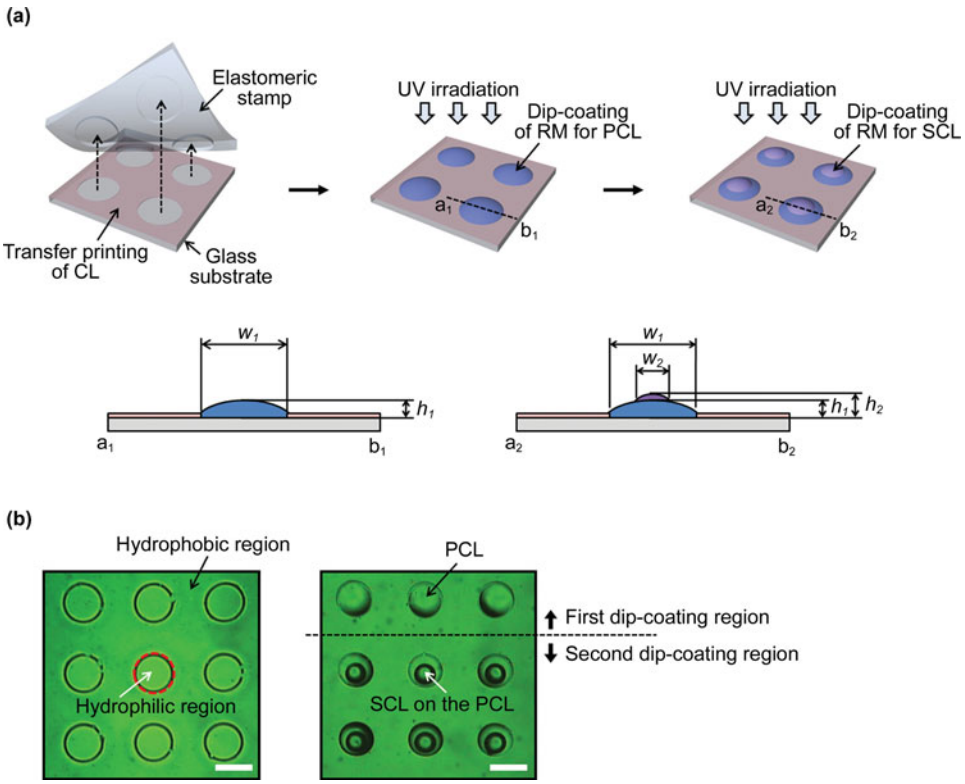

Figure 2. (a) The fabrication processes of the lens-on-lens and the side-views of the lenses. (b) Microscopic images showing the hydrophilic regions and the resultant SCL-on-PCL lens array. Scale bars are 200 μm.

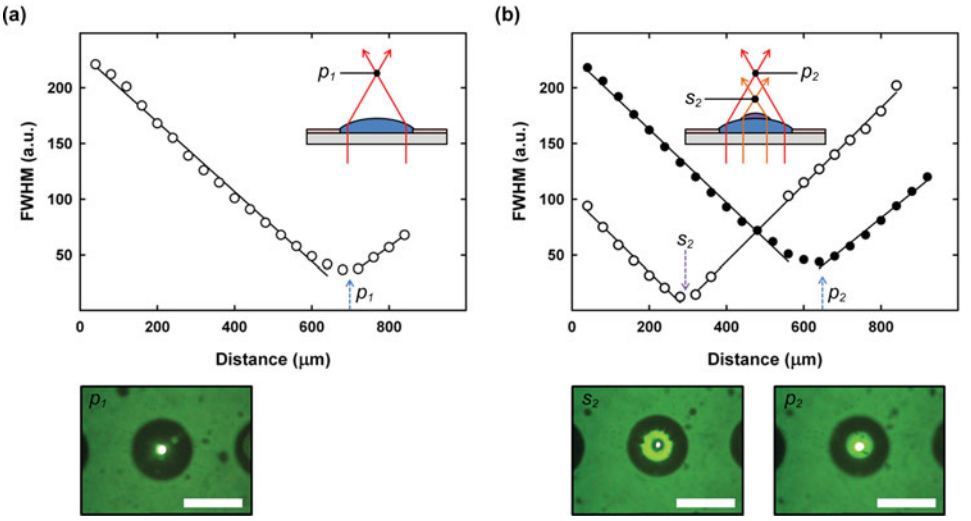

Figure 3. (a) FWHM of the light intensity for a single lens (PCL) as a function of the distance from the substrate and the microscope image focused at the focal plane p_1. (b) FWHM of the light intensity for the lens-on-lens (SCL-on-PCL) as a function of the distance from the substrate and the microscope images focused at the two focal planes of s_2 and p_2. Insets show the side-views of the lenses. Red and orange lines represent the light rays focused by the PCL and the SCL, respectively. Scale bars are 200 μm.

2. Experimental

The fabrication processes of our lens-on-lens architecture are described in Fig. 2. A fluorous-polymer (EGC-1700; 3M) was used as a commanding layer which transforms the surface to be ultra-hydrophobic so that a hydrophilic photo-reactive polymer layer was formed selectively on the substrate. As shown in Fig. 2(a), the hydrophilic circular regions surrounded by the ultra-hydrophobic region were first prepared on a glass substrate by transfer printing the fluorous-polymer with the help of an elastomeric stamp of poly(dimethylsiloxane) (GE Bayer Silicones). The PCL was then formed selectively on the glass substrate through the dip-coating process of the photo-reactive polymer NOA74 (Norland) at the speed of

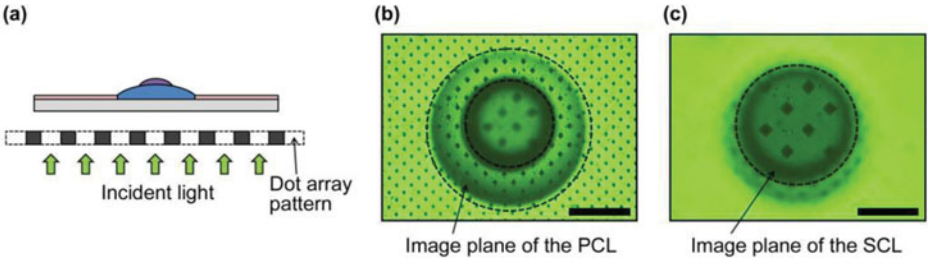

Figure 4. The image-depth representation capability of the lens-on-lens architecture: (a) the experimental geometry using an array of square patterns as an input image. The microscopic images of the square patterns observed through the lens-on-lens focused at (b) the image plane of the PCL and (c) the image plane of the SCL. Scale bars are 200 μm.

3 mm/s, followed by the UV irradiation at the intensity of 100 mW/cm^2 for 30 s for photo-polymerization. The SCL was precisely formed on the top of the PCL by simply repeating the dip-coating process and the UV irradiation. The width of the PCL, the height of the PCL, the width of the SCL, and the height of the lens-on-lens (SCL-on-PCL) architecture were denoted by w_1, h_1, w_2, and h_2, respectively, as shown in the side-views in Fig. 2(a). In fact, w_1 is determined by the size of the hydrophilic circular region and h_1 is governed by the dip-coating speed of the photo-reactive polymer due to the affinity of the photo-reactive polymer to the substrate but it becomes saturated above a certain value of the dip-coating speed. However, for the SCL, both w_2 and h_2 can be varied with the material viscosity and the dip-coating speed of the photo-reactive polymer. In our case, w_2 and h_2 were found to increase with increasing the dip-coating speed and the viscosity.

Figure 2(b) shows the microscope images of the hydrophilic regions and the resultant lens array. Clearly, each SCL was well-defined on the top of the PCL during the second dip-coating process. Note that the pattern resolution down to tens of micrometers can be easily achieved using the selective wetting technique. In addition, the achievable size of the SCL depends on the size of the PCL since the dip-coating speed of the photo-reactive polymer for the SCL should decrease with decreasing the PCL for partial wetting.

3. Results and Discussion

Let us first examine the full width half maximum (FWHM) of the light intensity for a single lens (PCL) and that for a lens-on-lens as a function of the distance from the substrate. In this experiment, the incident light whose central wavelength $\lambda = 532$ nm through a color filter was used for measuring the focal length of each lens. After passing through the lens, the light was collected using a charge-couple device (CCD) which was moved along the direction of the incident beam to determine the focal length of the lens. Figures 3(a) and 3(b) show the measured focal length of the single lens and that of the lens-on-lens, respectively. The images captured at three focal planes (at the points of p_1, p_2, and s_2) by the CCD were shown in Figs. 3(a) and 3(b). Clearly, the PCLs for the two lenses show similar focal lengths (at the points of p_1 and p_2) but the lens-on-lens has another focal length (at the point of s_2) originated from the SCL on the PCL.

Using the above lens-on-lens architecture, a simple image-depth representation was demonstrated in Fig. 4(a) where an array of square patterns was used as an input image. The square dot images focused at the image plane of the PCL and those of the SCL are shown in Figs. 4(b) and 4(c), respectively. It is clear that the lens-on-lens architecture is very useful for representing the image-depth.

4. Conclusion

We demonstrated a lens-on-lens architecture with two focal planes for image-depth representation. Two different focal lengths of the PCL and the SCL were realized by the difference between two geometrical curvatures produced through the selective wetting process. Our approach provides a simple and versatile platform to construct a variety of lens-on-lens arrays over large area for use in diverse optical systems.

References

[1] Takaki, Y., & Nago, N. (2010). *Opt. Express*, *18*, 8824.
[2] Zhao, W.-X., Wang, Q.-H., Wang, A.-H., & Li, D.-H. (2010). *Opt. Lett.*, *35*, 4127.

[3] Tolosa, A., Martínez-Cuenca, R., Pons, A., Saavedra, G., Martínez-Corral, M., & Javidi, B. (2010). *J. Opt. Soc. Am. A: Opt. Image. Sci. Vis.*, *27*, 495.
[4] Lim, Y.-T., Park, J.-H., Kwon, K.-C., & Kim, N. (2009). *Opt. Express*, *17*, 19253.
[5] Kim, Y., Park, J.-H., Choi, H., Jung, S., Min, S.-W., & Lee, B. (2004). *Opt. Express*, *12*, 421.
[6] Fujita, K., Nakamura, O., Kaneko, T., Oyamada, M., Takamatsu, T., & Kawata, S. (2000). *Opt. Commun.*, *174*, 7.
[7] Wu, L., & Xie, H. (2007). *IEEE/LEOS International Conference on Optical MEMS and Nanophotonics*, 141.
[8] Pan, C. T., Chen, M. F., Cheng, P. J., Hwang, Y. M., Tseng, S. D., & Huang, J. C. (2009). *Sensor. Actuat. A-Phys.*, *150*, 156.
[9] Masters, B. R. (1998). *Opt. Express*, *3*, 356.
[10] He, M., Yuan, X. C., Ngo, N. Q., Bu, J., & Kudryashov, V. (2003). *Opt. Lett.*, *28*, 731.
[11] Lu, Y., Yin, Y., & Xia, Y. (2001). *Adv. Mater.*, *13*, 34.
[12] Verma, A., & Sharma, A. (2010). *Adv. Mater.*, *22*, 5306.
[13] Ishii, Y., Koike, S., Arai, Y., & Ando, Y. (2000). *Jpn. J. Appl. Phys.*, *39*, 1490.
[14] MacFarlane, D. L., Narayan, V., Tatum, J. A., Cox, W. R., Chen, T., & Hayes, D. J. (1994). *IEEE Photon. Technol. Lett.*, *6*, 1112.
[15] Lim, C. S., Hong, M. H., Lin, Y., Xie, Q., Luk'yanchuk, B. S., Kumar, A. S., & Rahman, M. (2006). *Appl. Phys. Lett.*, *89*, 191125.
[16] Lee, S., Jeong, Y.-C., & Park, J.-K. (2007). *Opt. Express 15*, 14550.
[17] Chan, E. P., & Crosby, A. J. (2006). *Adv. Mater.*, *18*, 3238.
[18] Liu, K. H., Chen, M. F., Pan, C. T., Chang M. Y., & Huang, W. Y. (2010). *Sens. Actuators, A*, *159*, 126.
[19] Li, X., Ding, Y., Shao, J., Tian, H., & Liu, H. (2012). *Adv. Mater.*, *24*, OP165.
[20] Komma, Y., Tanaka, Y., Urairi, K., Nishino, S., & Mizuno, S. (1997). *Jpn. J. Appl. Phys.*, *36*, 474.
[21] Golub, M. A., Shurman, V., & Grossinger, I. (2006). *Appl. Opt.*, *45*, 144.
[22] Kim, H.-H., O, B.-H., Lee, S.-G., & Park, S.-G. (2010). *Microelectron. Eng.*, *87*, 1033.
[23] Leung, H. M., Zhou, G., Yu, H., Chau, F. S., & Kumar, A. S. (2009). *Appl. Opt.*, *48*, 5733.
[24] Lee, J.-M., Lee, D., & Baek, Y. (2013). *Opt. Commum.*, *289*, 69.
[25] Yu, H. B., Zhou, G. Y., Chau, F. K., Lee, F. W., Wang, S. H., & Leung, H. M. (2009). *Opt. Express*, *17*, 4782.
[26] Na, Y.-J., Lee, S.-W., Choi, W., Kim, S.-J., & Lee, S.-D. (2009). *Adv. Mater.*, *21*, 537.
[27] Choi, W., Kim, M.-H., & Lee, S.-D. (2011). *Jpn. J. Appl. Phys.*, *50*, 080219.